ARTICLE NO. 78-1626R

Simulation of Skylab Orbit Decay and Attitude Dynamics

Marshall H. Kaplan,* David J. Cwynar,† and Stephen G. Alexander†
The Pennsylvania State University, University Park, Pa.

Skylab offered a unique opportunity to develop simulations of both orbital decay and attitude motion of a large spacecraft with an opportunity for verification. Orbital decay data was readily available from tracking observations. Actual attitude motion was more difficult to observe. Scattered, brief sightings from ground-based telescopes offered limited data. Indirect methods involving drag calculations sometimes helped to confirm simulations. Such simulations were carried out for approximately two years before Skylab's re-entry. The fate of this large space station was sealed with the cancellation of the revisit mission in December 1978. Thus, during the last six months of its life, such simulations became important in order to aniticipate natural decay and attitude motion. This work led to possible schemes for shifting the re-entry time of Skylab through the technique of drag modulation.

I. Introduction

"SKYLAB is falling! Skylab is falling!" Chicken Little fans were chanting this all through the final months of Skylab's life. To date, over 6000 man-made orbiting objects have re-entered the atmosphere. Almost all have completely burned up before reaching the ground. One exception was Cosmos 954, the nuclear-powered Soviet satellite which re-entered on January 24, 1978, and scattered radioactive fragments over parts of Canada. Once the Skylab revisit mission was cancelled in December 1978, this too presented a threat of scattering fragments of metal over some region on the Earth. Fortunately, Skylab had no nuclear devices on board and the debris fell on an unpopulated area of Australia and in the Indian Ocean.

Up until the last two months of its life, Skylab's rate of descent was somewhat uncertain. Official estimates placed its re-entry anywhere between early-1979 and mid-1980. As it turned out, a shuttle revisit mission, which was planned for October 1979, would have been much too late to save Skylab. The space station fell to Earth on July 11, 1979. Its pieces melted and broke up such that debris was scattered over several thousands of square miles. No one will ever know exactly where all the pieces are, with the exceptions of those which fell in Australia.

Great concern over Skylab's potential risk led to a unique opportunity to develop and test simulations of its orbital decay and attitude dynamics. A great deal of knowledge related to large spacecraft resulted from this work. Orbit decay was modeled simply by subtracting the drag energy lost after each cycle about the Earth and converting this into an altitude reduction. Gravity gradient and atmospheric drag torques were modeled with greater difficulty to simulate uncontrolled, undamped attitude dynamics. Observational data assisted in verifying simulations. Applications of this technology to other spacecraft should be readily possible. A brief description of a technique involving reorientation of the spacecraft in order to modulate the drag is presented. This concept was in fact used during the last few orbits of Skylab's life.

Presented as Paper 78-1626 at the AIAA/IES/ASTM 10th Space Simulation Conference, Bethesda, Md., Oct. 16-18; submitted Dec. 1, 1978; revision received Sept. 13, 1979.

Index categories: Spacecraft Dynamics and Control; Spacecraft Simulation.

*Professor of Aerospace Engineering. Associate Fellow AIAA.
†Senior Research Technologist. Member AIAA.

The current interest in Skylab offers a unique opportunity to develop and test simulations of its orbital decay and attitude dynamics. A great deal of of new knowledge related to large spacecraft should result from the attempt to revisit our first space station. Orbit decay is modeled simply by subtracting the drag energy lost after each cycle about the Earth and converting this into an altitude reduction. Gravity-gradient and atmospheric drag torques are modeled with greater difficulty to simulate uncontrolled, undamped attitude dynamics. Observational data assist in verifying simulations. Applications of this technology to other spacecraft are speculated upon. Speculation is offered on the possibility of using a last-minute reorientation to move the expected footprint, should the revisit mission be cancelled.

II. Modeling for Simulation

Vehicle attitude dynamics are modeled via Euler's equations, as detailed in Ref. 1. This formulation is partially repeated here for convenience. Three coordinate systems come into play – body, inertial, and orbital. The body coordinate system is fixed to the spacecraft and rotates with it. Figure 1 illustrates these systems. Euler's equations are used here in the form[2]

$$\begin{aligned} I_x\dot{\omega}_x + (I_z - I_y)\omega_y\omega_y &= M_x \\ I_y\dot{\omega}_y + (I_x - I_z)\omega_x\omega_z &= M_y \\ I_z\dot{\omega}_z + (I_y - I_x)\omega_x\omega_y &= M_z \end{aligned} \tag{1}$$

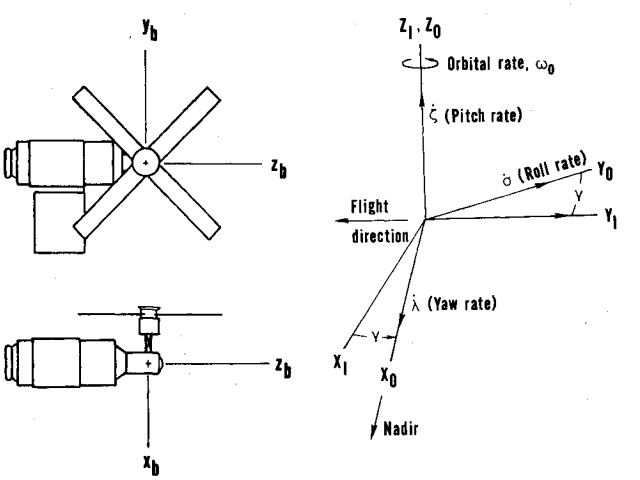

Fig. 1 Definition of coordinate systems used.

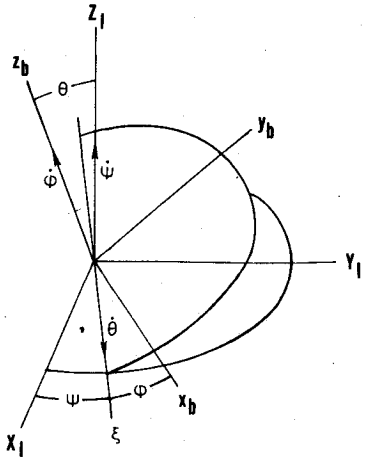

Fig. 2 Definition of Euler angles and rates.

where ω_x, ω_y, ω_z are the body angular velocities about x_b, y_b, z_b, respectively. M_x, M_y, M_z and I_x, I_y, I_z are the external torques and principal moments of inertia, respectively.

Internal damping was not modeled, because the time constant is thought to be several orbital periods. Driving torques act continuously and would not permit effective damping. Nevertheless, damping is important if Skylab were in an equilibrium orientation. As its altitude decreases, aerodynamic torques drive it away from equilibrium into a state of oscillation.

Since gravitational force acts in the orbital X_0 direction, a transformation is needed to express this force in the body frame. A typical Euler transformation is made between the body and the inertial coordinate systems,[1] as illustrated in Fig. 2. The only difference between the orbital and inertial frames is a rotation about the Z_o axis at the orbital rate, ω_o. Define the angle, γ, as the orbital position angle which is equal to $\int\omega_o dt$. Then define $\epsilon=\psi-\gamma$. The transformation matrix from the orbital to body coordinate system is then

$$\begin{bmatrix} x_b \\ y_b \\ z_b \end{bmatrix} = \begin{bmatrix} (C_\phi C_\epsilon - S_\phi C_\theta S_\epsilon) & (C_\phi S_\epsilon + S_\phi C_\theta C_\epsilon) & (S_\phi S_\theta) \\ (-S_\phi C_\epsilon - C_\phi C_\theta S_\epsilon) & (-S_\phi S_\epsilon + C_\phi C_\theta C_\epsilon) & (C_\phi S_\theta) \\ (S_\theta S_\epsilon) & (-S_\theta C_\epsilon) & (C_\theta) \end{bmatrix} \begin{bmatrix} X_o \\ Y_o \\ Z_o \end{bmatrix} \tag{2}$$

where $C_\phi=\cos\phi$, $S_\psi=\sin\psi$, etc. The large matrix can be represented by α, thus,

$$\begin{bmatrix} x_b \\ y_b \\ z_b \end{bmatrix} = \alpha \begin{bmatrix} X_o \\ Y_o \\ Z_o \end{bmatrix} \tag{3}$$

In addition to a coordinate transformation, one is needed between body rates and Euler rates. The Euler rates, $\dot{\psi}$, $\dot{\theta}$, $\dot{\phi}$, can be obtained by taking components of the body rates along the nonorthogonal axes,

$$\dot{\psi}=(\omega_y C_\phi+\omega_x S_\phi)/S_\theta$$

$$\dot{\theta}=\omega_x C_\phi-\omega_y S_\phi$$

$$\dot{\phi}=[-C_\theta(\omega_y C_\phi+\omega_x S_\phi)/S_\theta]+\omega_z$$

Orbital rates, referred to as the yaw rate ($\dot{\lambda}$), pitch rate ($\dot{\zeta}$), and roll rate ($\dot{\sigma}$), are

$$\begin{aligned} \dot{\lambda} &= \dot{\phi}S_\theta C_{(\pi/2-\psi+\gamma)}+\dot{\theta}C_{(\psi-\gamma)} \\ \dot{\sigma} &= \dot{\theta}C_{(\pi/2-\psi+\gamma)}-\dot{\phi}S_\theta C_{(\psi-\gamma)} \\ \dot{\zeta} &= \dot{\psi}+\dot{\phi}C_\theta-\omega_o \end{aligned} \tag{4}$$

Orbital angles, λ, σ, ζ, are obtained by integration of the associated rates, defined in Fig. 1. A gravity-gradient orientation is used as the initial state for some of the simulations presented here.

There are four potentially important environmental torques that act on a body in space. These are classified as aerodynamic, gravity-gradient, solar radiation, and magnetic. The inactive state and low orbit of Skylab leave only aerodynamic and gravity-gradient torques to be considered. Gravitational force acts in the direction of X_o since this axis always points toward nadir. The basic principle of gravity-gradient stabilization is that a body in a gravitational field, having one moment of inertia less than the other two, will experience a torque, tending to align the axis of least inertia with the field direction.[2] If $\vec{R}_o$ is the radius vector from the center of the Earth to the center of the orbital coordinate system, its components are easily determined in the body coordinate system using Eq. (3):

$$\begin{bmatrix} R_x \\ R_y \\ R_z \end{bmatrix} = \alpha \begin{bmatrix} -R_o \\ 0 \\ 0 \end{bmatrix}$$

or

$$\begin{aligned} R_x &= -R_o(C_\phi C_\epsilon - S_\phi C_\theta S_\epsilon) \\ R_y &= -R_o(-S_\phi C_\epsilon - C_\phi C_\theta S_\epsilon) \\ R_z &= -R_o S_\theta S_\epsilon \end{aligned} \tag{5}$$

Moments due to gravity-gradient torques about the body axes are obtained as

$$\begin{aligned} L_x &= (3\mu/R_o^5)R_z R_y(I_z-I_y) \\ L_y &= (3\mu/R_o^5)R_x R_z(I_x-I_z) \\ L_z &= (3\mu/R_o^5)R_x R_y(I_y-I_x) \end{aligned} \tag{6}$$

where μ is the gravitational constant of the Earth. These represent part of the inputs to Euler's equations. Moments due to the aerodynamic force must also be determined.

The orbital velocity vector, $\vec{V}_o$ is in the minus Y_o direction. Hence, components of velocity along the body axes are determined using Eq. (3):

$$\begin{bmatrix} V_x \\ V_y \\ V_z \end{bmatrix} = \alpha \begin{bmatrix} 0 \\ -V_o \\ 0 \end{bmatrix}$$

or, upon expansion,

$$\begin{aligned} V_x &= -V_o(C_\phi S_\epsilon + S_\phi C_\theta C_\epsilon) \\ V_y &= -V_o(-S_\phi S_\epsilon + C_\phi C_\theta C_\epsilon) \\ V_z &= +V_o S_\theta C_\epsilon \end{aligned} \tag{7}$$

Moments due to the aerodynamic forces about the body axes are determined from

$$\begin{aligned} A_x &= c_x q A_{\text{ref}} D_{\text{ref}} \\ A_y &= c_y q A_{\text{ref}} D_{\text{ref}} \\ A_z &= c_z q A_{\text{ref}} D_{\text{ref}} \end{aligned}$$

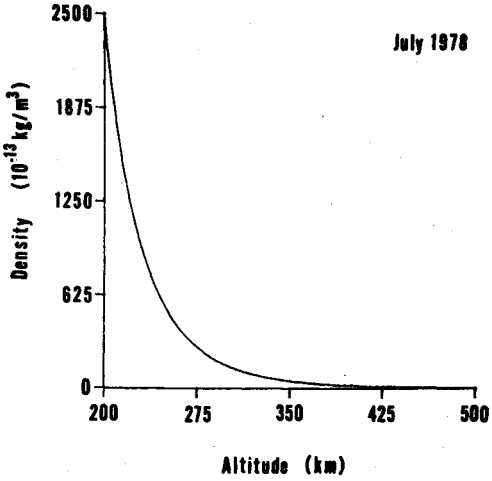

Fig. 3 Density as a function of altitude.

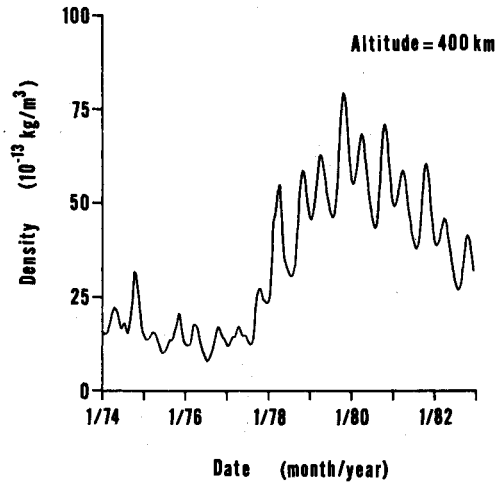

Fig. 4 Long-term density variations with time.

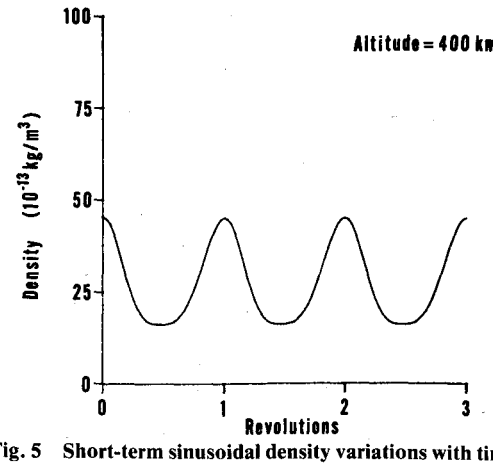

Fig. 5 Short-term sinusoidal density variations with time.

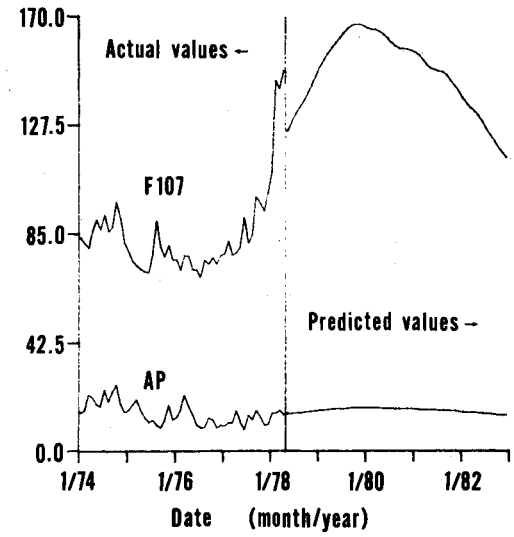

Fig. 6 F107 and AP variations with time.

where $q = \frac{1}{2}\rho V_o^2$, A_{ref} is the reference area and D_{ref} is the reference diameter. Determination of the atmospheric density, ρ, will be discussed later. The aerodynamic drag moment coefficients c_x, c_y, c_z were obtained from a NASA aerodynamic drag model. A Fourier series curve fit formula for c_x, c_y, c_z was derived as a function of the angle of attack, α_a and angle about the longitudinal axis, ϕ_a, of Skylab. These angles are computed as

$$\alpha_a = \cos^{-1}(V_z/V_o) \qquad 0 \text{ deg} \leq \alpha_a \leq 180 \text{ deg}$$
$$\phi_a = \tan^{-1}(V_y/-V_x) \qquad 0 \text{ deg} \leq \phi_a 360 \text{ deg}$$

The complete set of the moment components was used as input to Euler's equations. Thus, the right side of Eq. (1) consists of gravity-gradient and aerodynamic moments,

$$M_x = L_x + A_x$$
$$M_y = L_y + A_y$$
$$M_z = L_z + A_z \qquad (8)$$

Some data that are important in the preceding simulation was obtained from NASA. Skylab principal moments of inertia, about the body axes, have been calculated to be

$$I_x = 3{,}694{,}680 \text{ kg-m}^2$$
$$I_y = 3{,}767{,}828 \text{ kg-m}^2$$
$$I_z = 793{,}321 \text{ kg-m}^2$$

The mass of Skylab was estimated as $m = 77{,}111$ kg. The reference area and reference diameter used in aerodynamic force and moment modeling are[3] $A_{\text{ref}} = 79.86$ m^2 and $D_{\text{ref}} = 10.058$ m, respectively.

Tabulated values of drag coefficients for various orientations with respect to the flow were obtained from NASA.[3] The initial part of Skylab's decay trajectory, from January 1974 to June 1978, involves a passive vehicle with unknown orientation. Since the actual decay trajectory for this period was known, an average drag coefficient was determined by trial and error to be 5.2.

Atmospheric density is the most influential parameter with respect to the attitude and orbit decay of Skylab; thus, an accurate atmosphere model is an integral part of this investigation. It was found that a simple exponential function of altitude does not give accurate values of density at satellite heights. Above 125 km, density varies significantly with, not only altitude, but also with time in the form of solar and geomagnetic activities variations, seasonal variations, and diurnal variations. Ignoring these variations could cause as much as 200% error in atmospheric density calculations.

To account for density as a function of both altitude and time, a Jacchia (1970) atmosphere model was used.[4,5] The inputs required for the Jacchia routine are altitude, position (longitude and latitude), time (date and time of day), 10.7 cm solar flux (F107), and geomagnetic index (AP). The combination of the 10.7 cm solar flux and the geomagnetic index dictate what effect solar and geomagnetic activity will have on the upper atmosphere. The quantitative influence of this on atmospheric density will be discussed later.

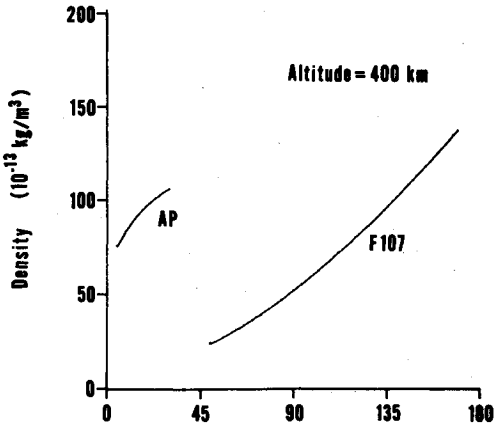

Fig. 7 Density variations with F107 and AP.

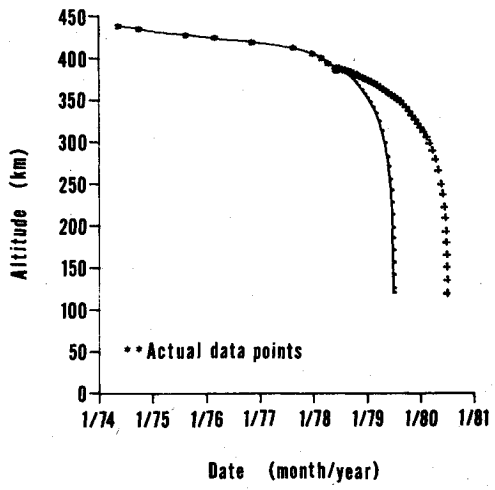

Fig. 8 Skylab orbital decay predictions.

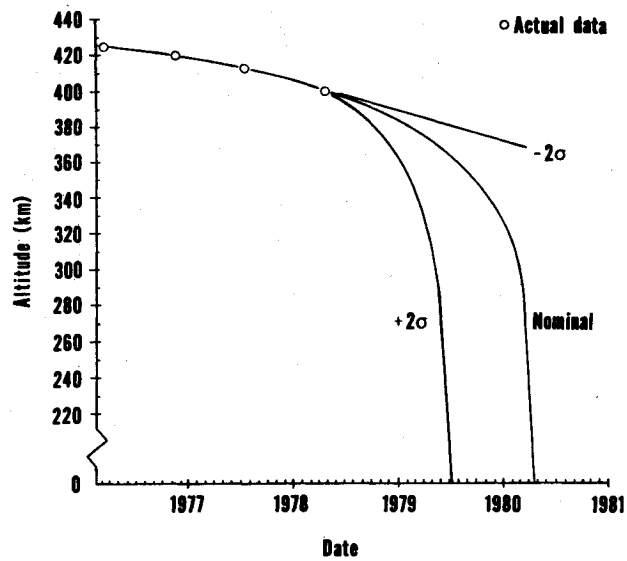

Fig. 9 NASA 1976 prediction of Skylab orbital decay.

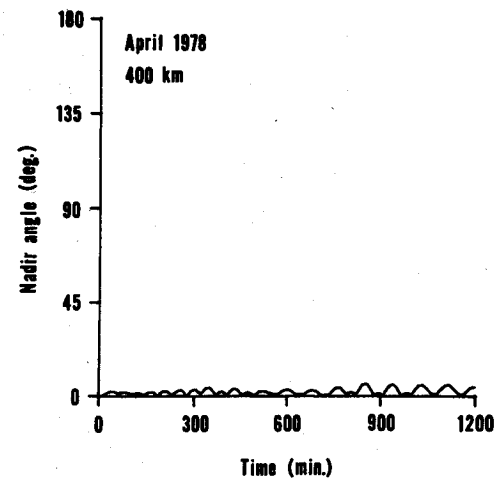

Fig. 10 Attitude motion for April 1978.

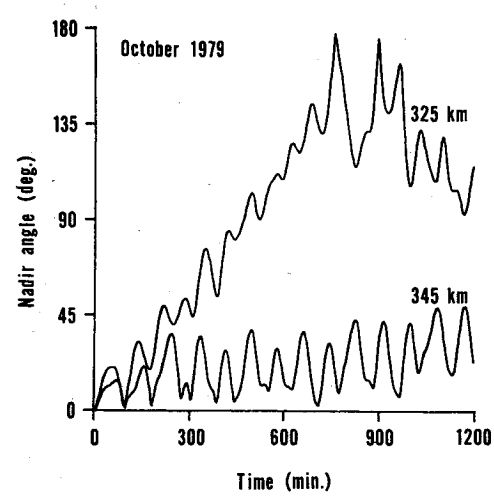

Fig. 11 Attitude motion for October 1979.

The density distributions computed by the Jacchia program are shown in Figs. 3-5. Figure 3 illustrates the expected exponential density curve with increasing altitude, with all time variations held constant. Long-term time variations in density at constant altitude are shown in Fig. 4, and variations during each orbit are depicted in Fig. 5. Variations are caused by solar and geomagnetic activity, as well as seasonal effects. The sinusoidal density distribution shown in Fig. 5 represents a short-term density variation, diurnal bulge, caused by thermal expansion effects on the sun-side of the Earth. This density distribution was used in the attitude simulation, while a combination of the distributions in Figs. 3 and 4 was incorporated into the orbit decay simulation in subroutine form.

Solar activity variations are predominantly caused by the 11-year solar cycle and associated sunspot activity (the current cycle will reach its maximum peak in mid-1979). Monthly averages of F107 and AP for the time period of interest are shown in Fig. 6.[6] Actual values are represented from January 1974 through April 1978, and the predicted values are shown for May 1978 to December 1982. The almost random fluctuations of the actual values of these two parameters reveals the uncertainty in the subsequent predicted values. To minimize this discrepancy, NASA Marshall Space Flight Center revises the F107 and AP predictions monthly. These revisions have been utilized in this investigation.

Even with the revisions, there still exists great uncertainty in the predictions of F107 and AP. Figure 7 shows the sensitivity of atmospheric density to changes in F107 and AP at an altitude of 400 km, as computed by the Jacchia (1970) programs. To obtain this plot, the Jacchia program was run with all variables held constant, while F107 and AP were separately varied from their minimum to maximum values, respectively. It is seen that accurate density calculations rely heavily on accurate predictions of F107 and AP.

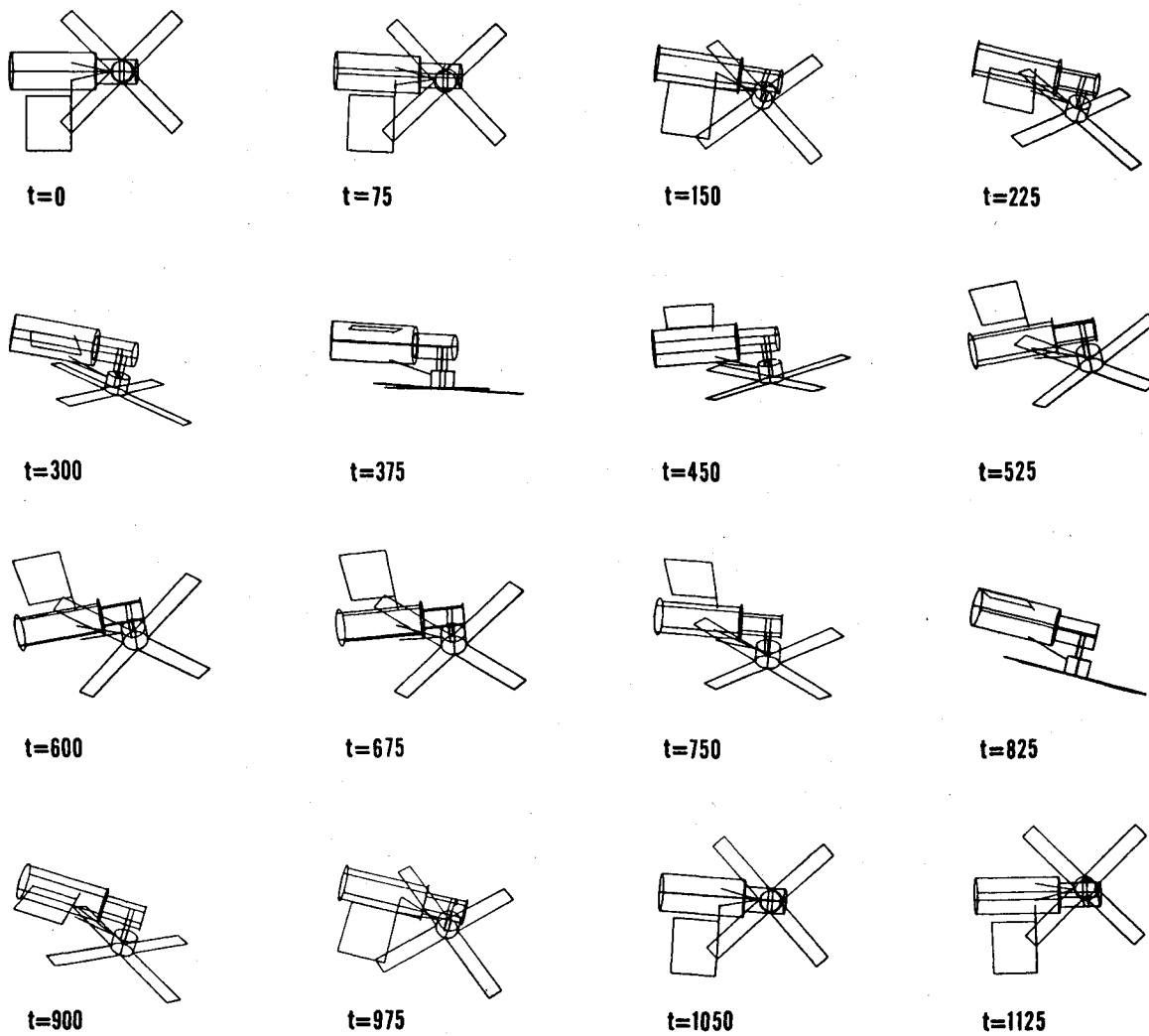

Fig. 12 Computer-drawn simulation of Skylab motion (t = time in minutes).

III. Orbit Decay Simulations

Skylab orbit decay was simulated using a discrete orbital energy dissipation model. A circular orbit approximation was assumed; therefore, the orbital energy per unit mass can be expressed as[2]

$$E = -\mu/2r \tag{9}$$

and the circular orbital velocity is

$$V_c = (\mu/r)^{1/2} \tag{10}$$

where r is the circular orbit radius. The aerodynamic drag force, D, acting on Skylab can be calculated from

$$D = \tfrac{1}{2} C_D \rho A_{\text{ref}} V_c^2 \tag{11}$$

where C_D, ρ, and A_{ref} are aerodynamic drag coefficient, local atmospheric density, and Skylab reference area, respectively. The power dissipated by this drag force is given as

$$P = DV_c = \tfrac{1}{2} C_D \rho A_{\text{ref}} V_c^3 \tag{12}$$

Now the incremental change in orbital kinetic energy dK, for a time span dt, is

$$dK = P\,dt \tag{13}$$

If, for a given time span, C_D, ρ, and V_c remain relatively constant, Eq. (13) becomes

$$\Delta K = P\Delta t \tag{14}$$

Thus, the new orbital energy per unit mass, E', is

$$E' = E - \Delta K/m \tag{15}$$

where m is the mass of Skylab. The resulting changes in orbital radius r', and velocity V_c', are

$$r' = -\mu/2E' \tag{16}$$

and

$$V_c' = (\mu/r')^{1/2} \tag{17}$$

This procedure can be iterated with the appropriate Δt to obtain an orbital decay trajectory.

Skylab orbit decay simulations were carried out on an IBM 370/168 digital computer. The starting date was May 14, 1974 when Skylab was last boosted to an altitude of 438 km. The initial time increment, Δt, was one day. To insure accurate density values in the final part of the decay, Δt was

automatically adjusted so that the altitude would not drop faster than 1 km/Δt.

In June 1978, NASA announced plans to attempt to increase the lifetime of Skylab. One option was the initiation of a general tumble mode which would reduce the average drag coefficient from the 5.2 of the passive orientation to 5.0. The second option involved an actively controlled reorientation with the Skylab longitudinal axis aligned with the orbital velocity vector. The resulting drag coefficient is 2.4, less than half that of the passive state. Both of these options were simulated from a starting date of June 11, 1978.

Figure 8 shows the results of the computer simulation. The solid line represents the case of passive orientation with re-entry in the late spring of 1979. The trajectory denoted by the dotted curve depicts the decay path had tumbling motion been initiated on June 11, 1978. It is seen that this would have increased the lifetime of Skylab by less than one month. The curve represented by the plus signs is for the controlled alignment option which was performed on June 11, 1978. This low-drag orientation should have extended Skylab's life into 1980. However, solar flare activity increased much faster than expected and this low-drag orientation only kept Skylab up until mid-1979.

IV. Attitude Dynamics Simulations

Attitude dynamics simulations were also done using the IBM 370/168 computer. The program uses a Hamming predictor-corrector method for integration. Due to the required accuracy, many of the runs used an excessive amount of computation time. Parameters varied, when doing the simulations, were orbital altitude and date. The sinusoidal density distribution described previously was used in these simulations, where each altitude/date point had a unique density amplitude and period.

NASA had provided a curve of anticipated orbital decay, dated November 1976, which permitted the generation of Fig. 9 with the associated 2σ deviations. The nominal curve predicts that the orbital altitude would have been 345 km if the revisit mission would have been carried out during late-1979. However, the decay rate did follow the $+2\sigma$ curve. A lower decay rate would have meant that a revisit mission might have been carried out.

Simulations were carried out assuming the nominal decay rate for different points in time between May 1979 and February 1980. Figure 10 shows the results for April 1978. The nadir angle is measured between the positive z_b axis and nadir. Thus, in April 1978, Skylab experienced an oscillation of less than 7 deg from the gravity-gradient orientation. Furthermore, simulations also indicate that angular rate and amplitude about the longitudinal z_b axis are very small. A simulation for an altitude of 345 km using the projected solar activity data for October 1979 resulted in the lower curve of Fig. 11. The vehicle was intially in a gravity-gradient orientation. This curve indicates that oscillatory motion with a 45 deg half-angle will be persistent. Angular rates associated with this motion are up to 5.4 deg/min. The upper curve of Fig. 11 shows the expected motion if Skylab's altitude was 20 km lower at mission time. The significance of this curve is that tumbling motion will occur even if the spacecraft is initially in a gravity-gradient orientation. In the actual case, of course, Skylab did go through a long period of reorientation before it re-entered. Had it been left alone to naturally find its own orientation, it is conceivable that Skylab could have reached a new equilibrium orientation with respect to a combination of gravity gradient and aerodynamic torques. Such a situation has been investigated, but the results are inconclusive. Different initial orientations were tried using perturbations associated with the atmospheric model near the re-entry date. Results indicated that a large amount of structural damping would have been required in order to reach a stable orientation.

Simulations were run for dates beginning about early-1977 and running through the re-entry date. Without structural damping, or other mechanisms for energy dissipation, these simulations indicated that the amplitude of oscillations away from nadir built up gradually. The implication of this is clear. If not actively controlled, Skylab would enter a state of general tumble. This, in fact, did happen in 1978.

A three-dimensional digital graphics program has been adapted for satellite simulation. The program uses the three-dimensional coordinates of the satellite to perform angular rotations prescribed by the attitude dynamics program. Figure 12 shows a frame-by-frame computer-drawn simulation of Skylab's motion for the 45 deg oscillations of Fig. 11.

V. Eleventh-Hour Contingency Plan

During the development of the simulation work in mid-1978, a concept of drag modulation was developed which might have permitted an eleventh-hour implementation of the plan to shift the re-entry point of Skylab. Even at that early date, it was clear that the shuttle revisit mission would probably be cancelled due to delays in the Space Shuttle program, accelerated decay due to increased solar flare activity, or the loss of Skylab's attitude control. Once its attitude control system was shut down, the spacecraft would enter a tumble as it descended. However, it seemed possible that increased aerodynamic torques would tend to stabilize Skylab sometime before its re-entry. Therefore, this contingency plan was studied and developed into a working concept. During the last few orbits of Skylab, the reaction control system would have been activated in order to cause Skylab to tumble. This would have only been done to further decrease the re-entry risk of the spacecraft. Such tumbling was thought to have been a way to decrease the life of Skylab by up to a few hours. The hypothesis was that natural stabilization would take place in such a way that Skylab's drag would be relatively low. With only approximately 500 lb-sec of propellant remaining in order to carry out a reorientation or tumble, any contingency plan would certainly be limited in its scope. In the actual case, a drag modulation scheme was carried out using continuous active attitude control to hold Skylab in a high-drag orientation. This was maintained until a few hours before re-entry. At that point Skylab's attitude control system was shut down and the spacecraft went into an uncontrolled tumble. It is believed that the timing of this tumble caused Skylab's life to be increased by approximately 18 minutes and prevented the spacecraft from skipping at the upper reaches of the atmosphere, thus preventing a re-entry far downstream from the expected point.

References

[1] Kaplan, M.H., Cwynar, D.J., and Alexander, S.G., "Anticipated Attitude Motion of Skylab for a 1979 Revisit Mission," *Journal of Spacecraft and Rockets,* Vol. 15, July-Aug. 1978, pp. 219-223.

[2] Kaplan, M.H., *Modern Spacecraft Dynamics and Control,* John Wiley, New York, 1976, Chaps. 1, 2, and 5.

[3] "Skylab-I Performance Data," NASA-MSC-01549, Vol. 4, Oct. 1972, pp. 9-54, 55, Appendices C-1, C-25.

[4] Justus, C.G., Woodrum, A.W., Roper, R.G., and Smith, O.E., "Four-D Global Reference Atmosphere Technical Description," Part I, NASA TM X-64871, Sept. 1974.

[5] Justus, C.G., Woodrum, A.W., Roper, R.G., and Smith, O.E., "Four-D Global Reference Atmosphere Users Manual and Programmers Manual," Part II, NASA-TMX 64872, Sept. 1974.

[6] Vaughan, W.W., "Solar Activity Indices and Predictions," NASA Marshall Space Flight Center, Memo dated Nov. 18, 1977.